

Incorporation of Copper Enhances the Anti-Ageing Property of Flame-Sprayed High-Density Polyethylene Coatings

Zhengmei Jia^{1,2} · Jing Huang¹ · Yongfeng Gong¹ · Peipeng Jin² · Xinkun Suo¹ · Hua Li¹

Submitted: 3 September 2016/in revised form: 26 October 2016
© ASM International 2017

Abstract High-density polyethylene (HDPE)-copper (Cu) composite coatings were prepared through depositing HDPE-Cu core-shell particles by flame spraying. The HDPE-Cu composite coatings and the HDPE coatings were aged in xenon lamp ageing testing chamber. The variations of chemical compositions and surface morphology of the coatings before and after the ageing testing were analyzed using infrared spectroscopy, scanning electron microscopy, thermogravimetric analysis, differential scanning calorimetry and ultraviolet-visible spectrophotometer. Results show that there is no chemical composition variation in the HDPE-Cu coatings. Cracks were found on the surfaces of the HDPE coatings, while the HDPE-Cu coating shows almost intact surface morphology. These results suggest that the HDPE-Cu coatings present better anti-ageing performances than the HDPE coatings. Further assessment of the function of Cu shells on the anti-ageing property reveals that Cu shells not only enhanced the absorption of the coatings to ultraviolet, but also increased their reflectivity to visible light. Additionally, the Cu shells enhanced the decomposition temperature and thermal stability of HDPE in the composite coatings. These results

give bright insight into potential anti-ageing applications of the polymer-based structures.

Keywords flame spraying · HDPE-Cu coatings · thermal analysis · UV ageing

Introduction

Marine corrosion environments are generally divided into atmospheric, splash, tidal, immersion and mud zones, and the protection to splash zone corrosion must be conducted with high priority. Steel structures in tidal zone usually suffer multi damnification, such as corrosion, biofouling, ageing, etc. With the development of the marine industry, corrosion and biofouling problems have drawn worldwide attentions, and many related investigations were reported in recent years (Ref 1, 2). To date, organic coatings are still the most popular protective layers against marine corrosion (Ref 1, 3-5). For antifouling coatings, copper agents including copper alloys, cuprous oxide and copper compounds have been used as principal biocides for decades. Copper-containing organic coatings have shown great potential in antifouling/anticorrosion applications (Ref 6-9). However, ageing of organic coatings is a main problem limiting their functional service duration (Ref 10), which usually results in degradation discoloration and brittle fracture (Ref 11, 12). Therefore, improvement of UV ageing resistance on the basis of increasing antifouling/anticorrosion performances of organic coatings is of great interest.

Many techniques have been attempted to fabricate metal/polymer composite coatings, such as painting, electroless plating, cold spraying, etc. However, it is noted that in these coatings, metal particles are dispersed in the

✉ Xinkun Suo
suoxinkun@gmail.com; suoxinkun@nimte.ac.cn

✉ Hua Li
lihua@nimte.ac.cn

¹ Key Laboratory of Marine Materials and Related Technologies, Zhejiang Key Laboratory of Marine Materials and Protective Technologies, Ningbo Institute of Materials Technology and Engineering, Chinese Academy of Sciences, Ningbo 315201, China

² Qinghai Provincial Key Laboratory of New Light Alloys, School of Mechanical Engineering, Qinghai University, Xining 810016, China

polymer matrix, and this structural feature cannot improve ageing resistance of the organic-based coatings. Therefore, a smart structure is expected, in which copper particles can not only play as biocide agent, but also protect organic matrix against ageing damage. Appropriate coating processes are to be explored for making the desirable structures.

Thermal spraying is an effective method for fabricating functional composite coatings, such as anticorrosion coatings (Ref 3, 13), antifouling coatings (Ref 14), antiwear coatings (Ref 3, 13, 15–17), weatherability coatings (Ref 18), antifriction coatings (Ref 16, 19), insulation coatings (Ref 20), high gloss coatings (Ref 20) and esthetic coatings (Ref 21). Compared to other coating methods, flame spraying is known for easy operation and cost efficiency in large-scale coating fabrication of vast variety of materials. In particular, flame spraying has been proven effective for making organic coatings, such as high-density polyethylene (HDPE) coatings, low-density polyethylene (LDPE) coatings, ultra-high molecular weight polyethylene (UHMWPE) coatings, and high-quality poly-ether-etherketone (PEEK) coatings (Ref 1, 3–5). In addition, as one of the most popular polymer materials, HDPE has been extensively used in various industries for example electronics, automobile and marine industries. The ageing property of HDPE was also drawn great attention (Ref 22–24). In this study, HDPE was selected as the typical organic matrix and copper particles were incorporated into the matrix to provide antifouling and anti-ageing effects. The smart structure was accomplished through feedstock powder preparation by electroless plating and coating fabrication by flame spraying. Chemical composition, microstructure and ageing-resistant property of the coatings were investigated and elucidated.

Materials and Methods

HDPE powder (Korea Petrochemical Ind. Co., Ltd) was used as the starting feedstock. The particles exhibit an ellipsoidal shape, and the particle size ranges from 54 to 140 μm with an average particle size of 85 μm . The HDPE particles were uniformly coated with Cu thin films through electroless plating. The plating was carried out through immersing the particles in an electroless plating bath for 40 min at 50 $^{\circ}\text{C}$. The schematic diagram of the powder pretreatment is shown in Fig. 1. The protocols employed for the powder pretreatment, including degreasing, coarsening, sensitizing and activating, were already established previously (Ref 25). The reagents used for the powder pretreatment were purchased (Sinopharm Chemical Reagent Co., Ltd., China) and used without any further purification. Mild steel plates (MS, E235B,

$20 \times 30 \times 2 \text{ mm}^3$) were used as the substrates. Prior to the spraying, the steel substrates were cleaned with acetone, hydrochloric acid and deionized water, and then mechanically coarsened by blasting alumina.

The HDPE-Cu powder was used as the feedstock for deposition of HDPE-Cu coatings using flame spraying (CDS 8000, Castolin, UK). Oxygen and acetylene were used as the combustion-supporting gas and the fuel gas with the pressure of 0.55 and 0.075 MPa, respectively. The powder feed rate was set as 60 g/min. The standoff distance from the nozzle exit to the sample surface was 250 mm. The traverse speed of the gun was 200 mm/s.

For assessment of the ageing performance, the HDPE coatings and HDPE-Cu composite coatings were placed in xenon lamp ageing testing chamber (ATLAS Ci4000, USA) for 7, 14 and 21 days. The ageing testing was carried out according to ASTM standard G26-C. The environmental temperature and humidity were set at $55 \pm 5 \text{ }^{\circ}\text{C}$ and $55 \pm 5\%$, respectively.

Chemical compositions of the coatings were examined using Fourier transform infrared spectrometry (FTIR, Nicolet 6700, Thermo Fisher Scientific, USA). The transmission mode was used in the wavenumber range of $400\text{--}4000 \text{ cm}^{-1}$. Cross-sectional and topographical morphology of the coatings was characterized by field emission scanning electron microscope (FESEM, Quanta FEG 250, USA). Differential scanning calorimetry and thermogravimetric analysis (DSC, TG/DTA, Perkin-Elmer, USA) were utilized to analyze the thermodynamic property of the powder and the coatings. TG/DTA was performed in nitrogen atmosphere with a heating rate of 10 $^{\circ}\text{C}/\text{min}$ from room temperature to 600 $^{\circ}\text{C}$. DSC analysis was conducted in nitrogen atmosphere with a heating rate of 10 $^{\circ}\text{C}/\text{min}$ from room temperature to 180 $^{\circ}\text{C}$. Two heating-up processes were employed to eliminate heat history of the coatings. The ultraviolet and visible spectrophotometer (Lambda 950, Perkin-Elmer, USA) was used to characterize the absorption in a range of 200–800 nm.

Results and Discussion

The HDPE particles were uniformly coated with Cu thin films after the electroless plating, and the cross-sectional view of individual HDPE-Cu particle evidences the enwrapped structural feature (Fig. 2a). The HDPE particles are entirely wrapped by thin copper layers. The HDPE-Cu core-shell structures were used to fabricate composite coatings using flame spraying. The coatings were cut, mounted and polished for observing their cross-sectional microstructures, which are shown in Fig. 2(b) and (c). It can be found that no apparent defects such as microcracks and pores are found in both the HDPE coatings and the

Fig. 1 Schematic diagram of the electroless plating processing route for making the HDPE-Cu particles

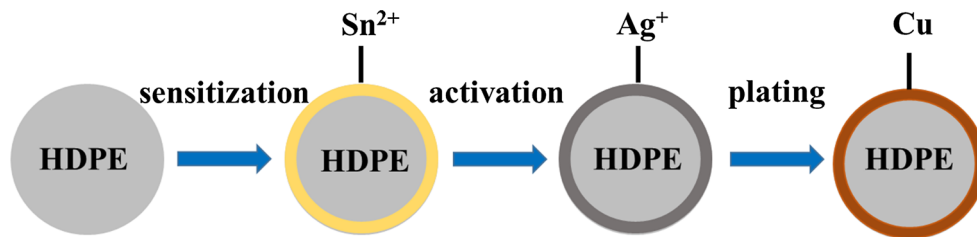
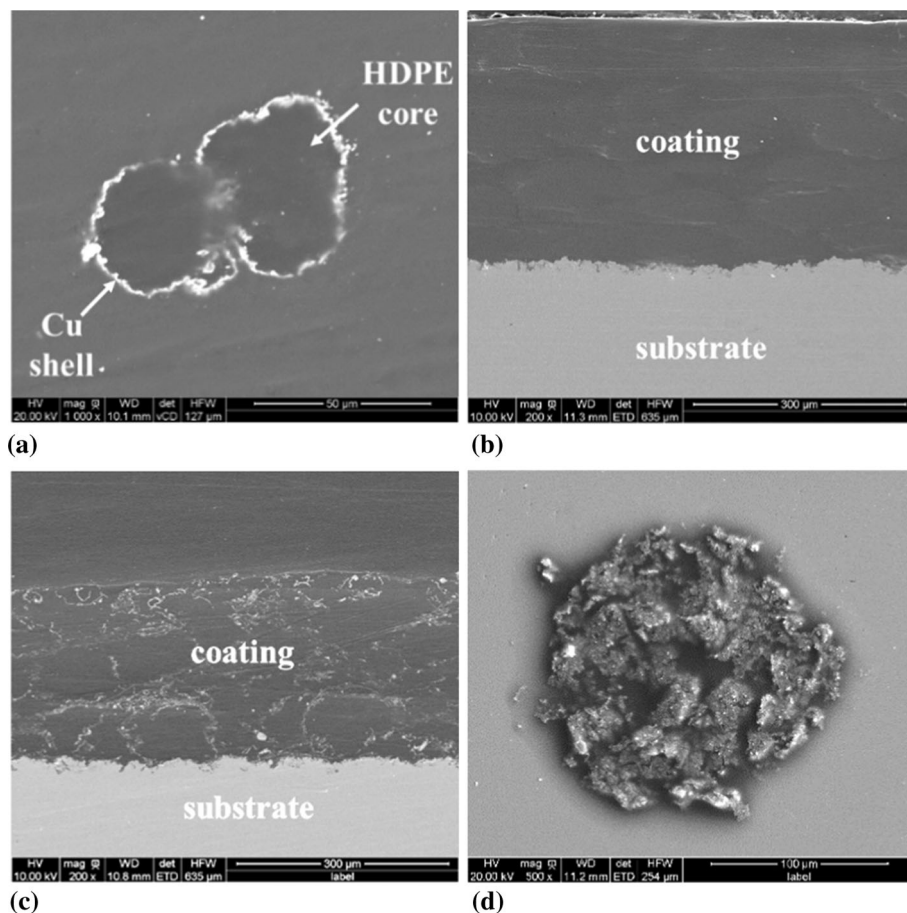


Fig. 2 Cross-sectional microstructures of the HDPE-Cu particle (a), the HDPE coating (b), and the HDPE-Cu composite coating (c), and the surface morphology of the HDPE-Cu splat (d)



HDPE-Cu coatings. In addition, no delamination is observed at the interface between the coating and the substrate. It is also clear that Cu distributes homogeneously in the HDPE-Cu coatings (Fig. 2c). Similar to the Cu-coated HDPE particles, the Cu element also sites along the boundary of the HDPE particle in the composite coating, although the composite particles experienced softening and deformation during spraying. To further elucidate the flattening behavior of the HDPE-Cu particles, individual splats were collected and characterized (Fig. 2d). The black contrast zone is identified as the polymer, and the gray/white contrast zone is identified as Cu. It is clear that the Cu shell that wraps the HDPE core before spraying keeps adhering on the flattened HDPE. Compared to the starting HDPE-Cu particles which show continuous

enwrapping state of the Cu shell, the splat exhibits slightly discontinuous lamella structure of the Cu layer, which is likely attributed to deformation of the composite particle upon the impingement.

The heating state of in-flight HDPE particles and HDPE-Cu particles was further investigated by TG/DSC analysis. The thermal parameters of the powder and the coatings are shown in Table 1. $T_{5\%}$ refers to the temperature at 5% weight loss of the composite coating, and $T_{d(max)}$ is assigned to the maximum decomposition temperature of the coating. It is realized that the crystallinity of HDPE in the coating significantly augments compared to that in the starting HDPE powder regardless if the HDPE particles or the HDPE-Cu particles are tested, suggesting that both HDPE particles and HDPE-Cu particles experienced full

melting in flame. This is consistent with the morphological observation of the HDPE-Cu splats (Fig. 2d) that full melt state was attained for the particles.

For the ageing testing, the HDPE coatings and the HDPE-Cu coatings were placed in the UV ageing chamber for 7, 14 and 21 days. The surface color changes of the samples during the accelerated ageing were observed, and the results are shown in Fig. 3. It is found that the original HDPE surface presents a black contrast. As the HDPE coatings were placed in the ageing chamber for 7 days, some white speckles were observed on the coating surfaces. The change in color relates to the change of polymer chain structure (Ref 26). As the ageing time was elongated to 14 days, the area of the white speckles increased from 1.16 ± 0.37 to $11.28 \pm 1.29\%$. As the ageing time increased to 21 days, the area of the white speckles increased to $39.15 \pm 4.44\%$. It was reported that the albi-fication of HDPE was involved in the photooxidation of polymer, which resulted in shortening of molecular chain (Ref 23). Different from the HDPE coatings, the HDPE-Cu coatings did not present any change in their surface color, indicating much better anti-ageing performances.

Apart from the surface color observation of the coatings, the surface morphology of the coatings was also

characterized using SEM. Figure 4 shows the evolution of the surface morphology of the HDPE coatings and the HDPE-Cu composite coatings as a function of ageing time. The surfaces of the HDPE coatings before the ageing testing present a flat and compact feature (Fig. 4a-1). After the ageing testing, the coatings tend to exhibit remarkably different morphology (Fig. 4a-2, a-3, and a-4). Deep cracks are shown on the surfaces of the HDPE coatings after the ageing. Intensified cracks are seen for the HDPE coatings with further elongated ageing and the cracks become interlinked. By contrast, the HDPE-Cu composite coatings do not exhibit perceptible variation in surface morphology even after 21 days of ageing (Fig. 4b). The heterophany in surface morphology of the samples before and after the ageing testing is likely attributed to ageing-induced degradation of the polymer.

Changes in chemistry of HDPE were characterized by infrared spectrometry (IR), which is usually used to investigate the chemical information such as molecular bonds or vibrations of organic compounds (Ref 27, 28). Figure 5 presents the IR spectra of the HDPE coatings and the HDPE-Cu composite coatings before and after the ageing. In Fig. 5(a), six vibrational bands can be found at 2927 , 2853 , 1475 , 1374 and 733 cm^{-1} , which correspond

Table 1 Thermal parameters of the powder and the coatings

Samples	T_m , °C	$T_{5\%}$, °C	$T_{d(\text{max})}$, °C	ΔH_m , J g ⁻¹	χ_c , %
HDPE powder	132.2	395.4	462.7	142.1	52.6
HDPE-Cu powder	132.4	408.7	474.8	103.3	38.2
HDPE coating	126.5	390.9	467.4	168.3	57.4
HDPE-Cu coating	130.1	376.3	461.5	168.5	63.9

T_m , melting temperature; $T_{5\%}$, temperature at 5% weight loss; $T_{d(\text{max})}$, maximum decomposition temperature; ΔH_m , melting enthalpy; and χ_c , degree of crystallinity of HDPE

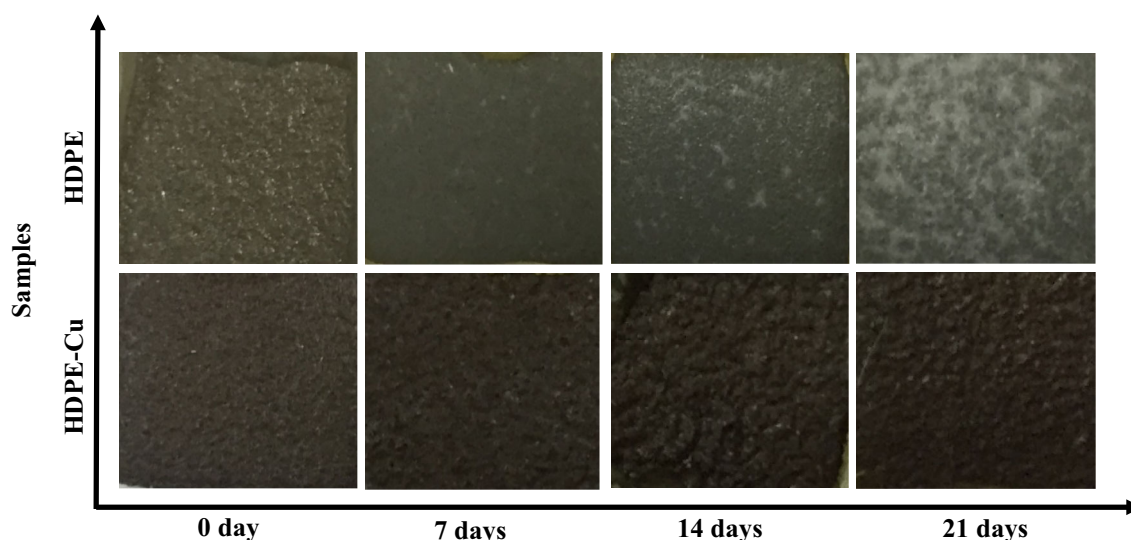


Fig. 3 Surface color evolution of the HDPE coating and the HDPE-Cu coating as a function of ageing time

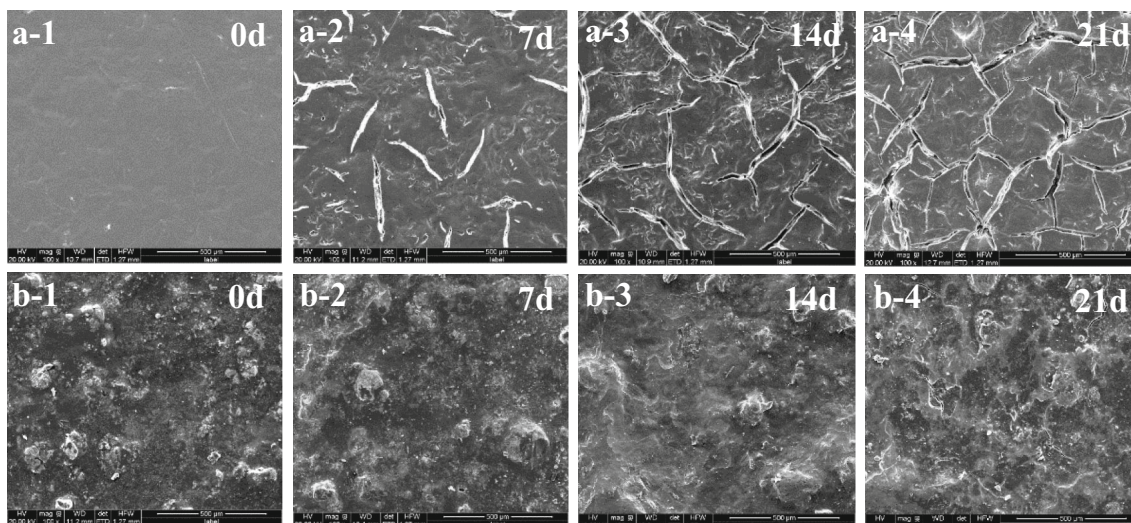


Fig. 4 Surface morphology evolution of the HDPE coating (a-1, a-2, a-3, a-4) and the HDPE-Cu coating (b-1, b-2, b-3, b-4) as a function of ageing time

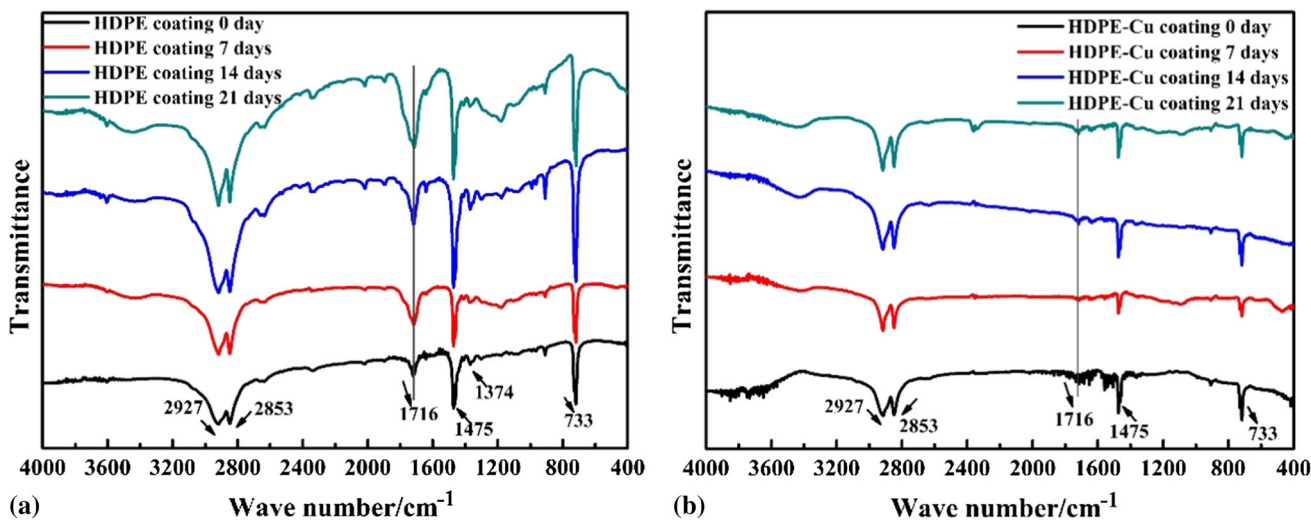


Fig. 5 FTIR spectra of the HDPE coating (a) and the HDPE-Cu composite coating (b)

to anti-symmetrical stretching vibration peak, symmetrical stretching vibration peak, scissoring peak, symmetrical deformation stretching vibration peak, resonance absorption peak of carbon-hydrogen bond (C-H) in HDPE, respectively. It is worth noting that the vibrational band at 1716 cm⁻¹ is not the characteristic absorption band of HDPE, but the stretching vibration peak of carbonyl group (C=O). The carbonyl group in HDPE is presumably attributed to the photooxidation reaction of the polymer. In addition, the intensity of the carbonyl group increases with the increase of the accelerated ageing time, suggesting aggravated degradation of HDPE as the ageing time increases. The IR spectra of the HDPE-Cu composite coatings (Fig. 5b) does not show the peaks for carbonyl

group, suggesting that HDPE in the composite coatings did not experience photodegradation. The IR results suggest that the presence of copper in the HDPE-based coatings improves their ageing-resistant property.

To clarify the effect of the incorporation of copper on the anti-ageing performances of the coatings, UV shielding ability of the coatings was examined. Figure 6 shows the UV absorption spectra of the coatings. The absorbance peak of the HDPE coatings in the visible region (400-800 nm) is higher than that of the HDPE-Cu coatings. This suggests that copper located in between HDPE splats enhances the reflectivity of the coatings, accordingly reduces their absorption to visible light. Furthermore, the UV absorbance intensity of the HDPE-Cu composite

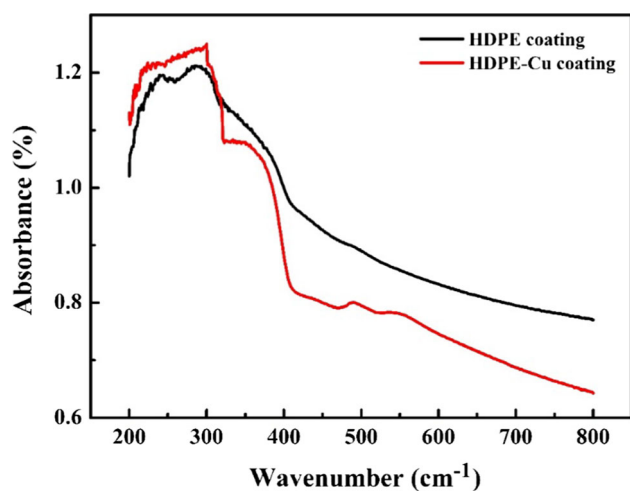


Fig. 6 UV-Vis absorption spectra of the coatings

coatings is higher than that of the HDPE coatings in the wavelength range of 200–300 nm, suggesting that the absorbance to UV of the Cu shells is better than that of the polymer.

TG and DSC analyses were also conducted to elucidate the function of the Cu shells on the ageing resistance of the HDPE-based composites. TG curves of the coatings are shown in Fig. 7(a) and (b). It is found that the initial decomposition temperature, also called as the 5% weight loss temperature of the HDPE coatings (366.1 °C), is lower than that of the HDPE-Cu composite coatings after the accelerated ageing test for 21 days (382.3 °C). The decrease of the initial decomposition temperature is likely due to rupture of molecular chains in HDPE. Figure 7(c) and (d) shows the DSC results of the HDPE coatings and the HDPE-Cu coatings during the

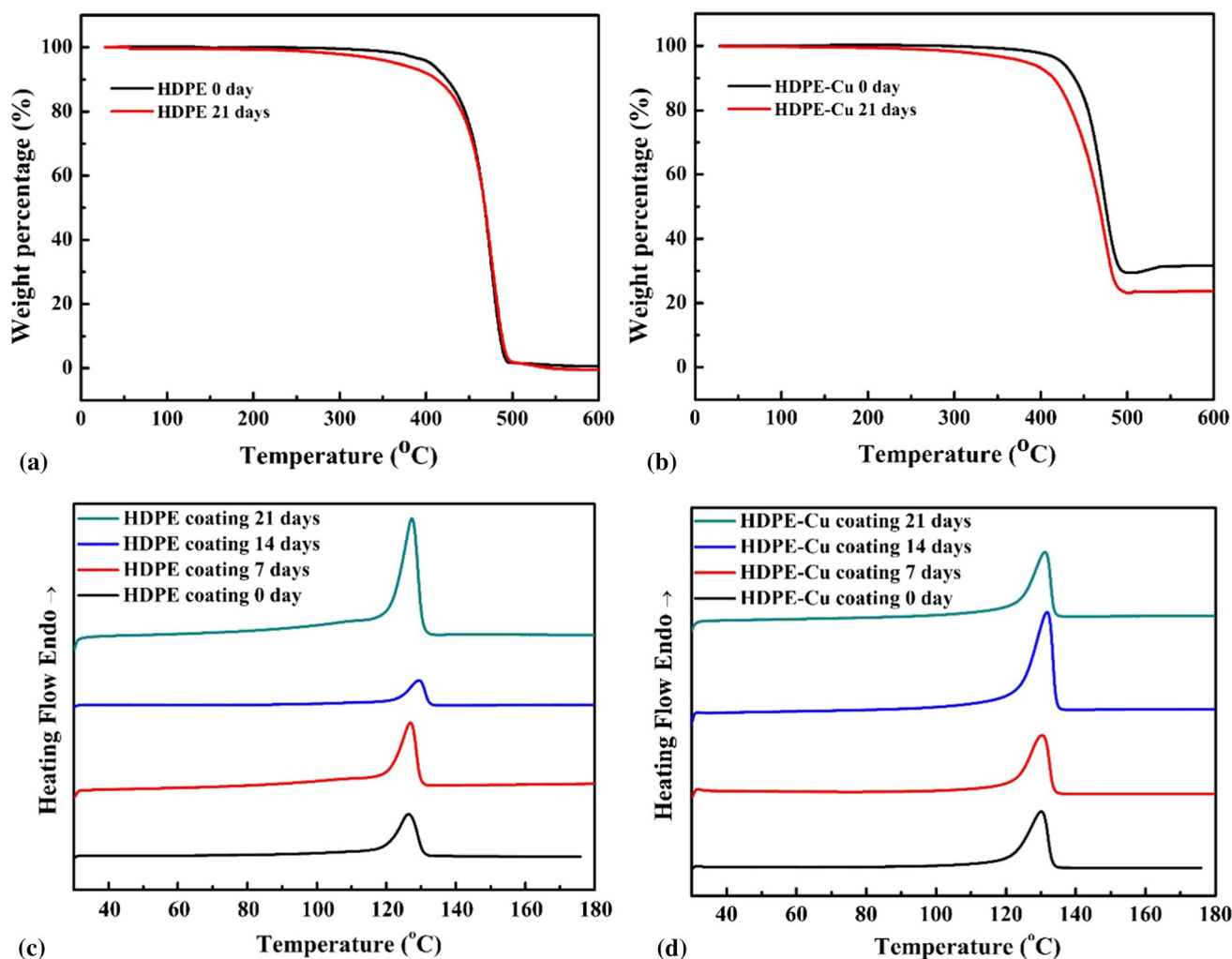


Fig. 7 TG curves of the HDPE coating (a), the HDPE-Cu coating (b) and DSC curves of the HDPE coating (c), the HDPE-Cu coating (d) before and after ageing test

Table 2 Thermal parameters acquired from DSC analyses of the HDPE coating

Time, d	T_m , °C	ΔH_m , J g ⁻¹	χ_c , %
0	126.5	168.3	57.4
7	126.9	134.6	45.9
14	129.5	110.7	37.8
21	127.5	98.1	33.5

Table 3 Thermal parameters acquired from DSC analyses of the HDPE-Cu coating

Time, d	T_m , °C	ΔH_m , J g ⁻¹	χ_c , %
0	130.1	168.5	63.9
7	130.5	165.3	62.7
14	131.8	142.2	53.9
21	131.2	122.6	46.5

T_m , melting temperature; ΔH_m , melting enthalpy; and χ_c , degree of crystallinity

ageing testing. The thermal parameters including crystallinity (X_c), melting temperature (T_m) and enthalpy change (ΔH_m) of the coatings are summarized in Tables 2 and 3, respectively. It is clear that the melting temperature of the coatings did not vary as a function of the ageing time. It is also found that the melting temperature of the HDPE-Cu coatings is always higher than that of the HDPE coatings. The crystallinity degree of the polymer can be calculated using the formula (Ref 29): $X_c = \Delta H_m(T_m) / \Delta H_m^\circ(T_m^\circ)$, where $\Delta H_m(T_m)$ and $\Delta H_m^\circ(T_m^\circ)$ are the melting enthalpy and the melting enthalpy with a crystallinity of 100%, respectively. The melting enthalpy of HDPE with a crystallinity of 100% is 293 J/g (Ref 30). As shown in Tables 2 and 3, the melting enthalpy and the crystallinity of the coatings decrease with the increase of the ageing time. However, the decrease amplitude in melting enthalpy and crystallinity of the HDPE-Cu coatings is significantly lower than that of the HDPE coatings. The melting enthalpy is related to molecular weight of the polymer. Based on the thermal analyses, it can be concluded that the Cu inclusion increases the initial decomposition temperature and the melting temperature of HDPE in the coatings, resulting in enhanced anti-ageing performances.

Conclusions

HDPE coatings and HDPE-Cu composite coatings were fabricated by flame spraying. The coatings were aged in a xenon lamp ageing chamber for 7, 14 and 21 days to evaluate the effect of Cu inclusion on their anti-ageing

properties. The HDPE-Cu composite coatings present excellent ageing-resistant performances. The incorporation of Cu enhances remarkably the ultraviolet absorption intensity of the HDPE-based coatings. In addition, the Cu inclusion increases the visible light reflectivity of the coatings and increases initial decomposition temperature and melting temperature of HDPE in the coatings. The results would give insight into design and thermal spray fabrication of polymer/metal composite coatings for a variety of applications.

Acknowledgments This work was supported by Project of Scientific Innovation Team of Ningbo (2015B11050), National Natural Science Foundation of China (31500772 and 41476064), Key Research and Development Program of Zhejiang Province (2015C01036), International Scientific and Technological Cooperation Project of Ningbo (2016D10012) and 3315 Program of Ningbo.

References

- K.J. Jothi, A.U. Santhoskumar, S. Amanulla, and K. Palanivelu, Thermally Sprayable Anti-corrosion Marine Coatings Based on MAH-g-LDPE/UHMWPE Nanocomposites, *J. Therm. Spray Technol.*, 2014, **23**, p 1413-1424
- P. Buskens, M. Wouters, C. Rentrop, and Z. Vroon, A Brief Review of Environmentally Benign Antifouling and Foul-Release Coatings for Marine Applications, *J. Coat. Technol. Res.*, 2013, **10**, p 29-36
- C.R.C. Lima, N.F.C. de Souza, and F. Camargo, Study of Wear and Corrosion Performance of Thermal Sprayed Engineering Polymers, *Surf. Coat. Technol.*, 2013, **220**, p 140-143
- A. Soveja, P. Sallamand, H.L. Liao, and S. Costil, Improvement of Flame Spraying PEEK Coating Characteristics Using Lasers, *J. Mater. Process. Technol.*, 2011, **211**, p 12-23
- C. Zhang, G. Zhang, V. Ji, H.L. Liao, S. Costil, and C. Coddet, Microstructure and Mechanical Properties of Flame-Sprayed PEEK Coating Remelted by Laser Process, *Prog. Org. Coat.*, 2009, **66**, p 248-253
- P.C. King, A.J. Poole, S. Horne, R. de Nys, S. Gulizia, and M.Z. Jahedi, Embedment of Copper Particles into Polymers by Cold Spray, *Surf. Coat. Technol.*, 2013, **216**, p 60-67
- M.J. Vucko, P.C. King, A.J. Poole, C. Carl, M.Z. Jahedi, and R. de Nys, Cold Spray Metal Embedment: An Innovative Antifouling Technology, *Biofouling*, 2012, **28**, p 239-248
- M.J. Vucko, P.C. King, A.J. Poole, Y. Hu, M.Z. Jahedi, and R. de Nys, Assessing the Antifouling Properties of Cold-Spray Metal Embedment Using Loading Density Gradients of Metal Particles, *Biofouling*, 2014, **30**, p 651-666
- M.J. Vucko, P.C. King, A.J. Poole, M.Z. Jahedi, and R. de Nys, Polyurethane Seismic Streamer Skins: An Application of Cold Spray Metal Embedment, *Biofouling*, 2013, **29**, p 1-9
- H. Wu, L. Li, J.Y. Yu, S. Xu, and D. Xie, Effect of Layered Double Hydroxides on Ultraviolet Aging Properties of Different Bitumens, *Constr. Build. Mater.*, 2016, **111**, p 565-570
- L. Rosu, C.N. Cascaval, C. Ciobanu, D. Rosu, E.D. Ion, C. Morosanu, and M. Enachescu, Effect of UV Radiation on the Semi-interpenetrating Polymer Networks Based on Polyurethane and Epoxy Maleate of Bisphenol A, *J. Photochem. Photobiol. A Chem.*, 2005, **169**(2), p 177-185
- K.A.M. dos Santos, P.A.Z. Suarez, and J.C. Rubim, Photo-Degradation of Synthetic and Natural Polyisoprenes at Specific UV Radiations, *Polym. Degrad. Stab.*, 2005, **90**(1), p 34-43

13. C.R.C. Lima, N.F.C. de Souza, and F. Camargo, Study of the Characteristics of Thermally Sprayed Polymer Coatings for Wear and Corrosion Protection of Metallic Substrates, *Soldag. Insp.*, 2012, **17**(4), p 369-375
14. R. Ding, X. Li, J. Wang, and L. Xu, Study on Antifouling Effect of Cold Spray Cu-Cu₂O Coating, *Paint Coat. Ind.*, 2013, **43**, p 1-6
15. T. Fender, Thermal Spray High Performance Polymer Coatings, *Mater. Technol.*, 1996, **11**(1), p 16-20
16. M. Yamane, T.A. Stolarski, and S. Tobe, Wear and Friction Mechanism of PTFE Reservoirs Embedded into Thermal Sprayed Metallic Coatings, *Wear*, 2007, **263**, p 1364-1374
17. R.A.X. Nunes, W. Sade, and J.R.T. Branco, Friction and Wear of a Thermal Sprayed PET-Poly(Ethylene Teraphthalate) Coating, *Polimeros*, 2007, **17**(3), p 244-249
18. S. Rossi, M. Fedel, S. Petrolli, and F. Deflorian, Accelerated Weathering and Chemical Resistance of Polyurethane Powder Coatings, *J. Coat. Technol. Res.*, 2016, **13**(3), p 427-437
19. A. Rempp, A. Killinger, and R. Gadow, New Approach to Ceramic/Metal-Polymer Multilayered Coatings for High Performance Dry Sliding Applications, *J. Therm. Spray Technol.*, 2012, **21**(3-4), p 659-667
20. Y.C. Zhuang, D.Q. Yu, F.W. Dai, G.P. Zhang, and J. Fan, Spray Coating Process with Polymer Material for Insulation in CIS-TSV Wafer-Level-Packaging, *2014 15th International Conference on Electronic Packaging Technology (Icept)*, 2014, p 437-440
21. T.A. Misev and R. van der Linde, Powder Coatings Technology: New Developments at the Turn of the Century, *Prog. Org. Coat.*, 1998, **34**(1-4), p 160-168
22. S.S. Ting, N.K. Achmad, H. Ismail, R. Santiagoo, and N.N. Zulkepli, Thermal Degradation of High-Density Polyethylene/Soya Spent Powder Blends, *J. Polym. Eng.*, 2015, **35**(5), p 437-442 ([in English])
23. A.M.R. Ewais and R.K. Rowe, Effect of Aging on the Stress Crack Resistance of an HDPE Geomembrane, *Polym. Degrad. Stab.*, 2014, **109**, p 194-208 ([in English])
24. R.K. Rowe, F.B. Abdelaal, and M.Z. Islam, Aging of High-Density Polyethylene Geomembranes of Three Different Thicknesses, *J. Geotech. Geoenviron. Eng.*, 2014, **140**(5), p 11 ([in English])
25. M. Narkis, J. Yacubowicz, A. Vaxman, and A. Marmur, Electrically Conductive Composites Prepared from Polymer Particles Coated with Metals by Electroless Deposition, *Polym. Eng. Sci.*, 1986, **26**, p 139-143
26. R.S.C. Woo, Y. Chen, H. Zhu, J. Li, J.K. Kim, and C.K.Y. Leung, Environmental Degradation of Epoxy-Organoclay Nanocomposites Due to UV Exposure. Part I: Photo-Degradation, *Compos. Sci. Technol.*, 2007, **67**(15-16), p 3448-3456
27. B.F. Bowers, B. Huang, and X. Shu, Refining Laboratory Procedure for Artificial RAP: A Comparative Study, *Constr. Build. Mater.*, 2014, **52**, p 385-390
28. B.F. Bowers, B. Huang, X. Shu, and B.C. Miller, Investigation of Reclaimed Asphalt Pavement Blending Efficiency Through GPC and FTIR, *Constr. Build. Mater.*, 2014, **50**, p 517-523
29. W. Balcerowiak, The Degree of Crystallinity of Polymer Systems as Determined by DSC, *Polimery*, 1998, **43**(6), p 373-378
30. S. Mir, T. Yasin, P.J. Halley, H.M. Siddiqi, and T. Nicholson, Thermal, Rheological, Mechanical and Morphological Behavior of HDPE/Chitosan Blend, *Carbohydr. Polym.*, 2011, **83**(2), p 414-421